



**HAL**  
open science

## Time-dependent methodology for non-stationary mass flow rate measurements in a long micro-tube

Marcos Rojas-Cárdenas, Ernane Silva, Minh-Tuan Ho, César Deschamps,  
Irina Martin Graur

► **To cite this version:**

Marcos Rojas-Cárdenas, Ernane Silva, Minh-Tuan Ho, César Deschamps, Irina Martin Graur. Time-dependent methodology for non-stationary mass flow rate measurements in a long micro-tube. *Microfluidics and Nanofluidics*, 2017, 21 (5), pp.86. 10.1007/s10404-017-1920-9 . hal-01835712

**HAL Id: hal-01835712**

**<https://hal.science/hal-01835712v1>**

Submitted on 24 Dec 2019

**HAL** is a multi-disciplinary open access archive for the deposit and dissemination of scientific research documents, whether they are published or not. The documents may come from teaching and research institutions in France or abroad, or from public or private research centers.

L'archive ouverte pluridisciplinaire **HAL**, est destinée au dépôt et à la diffusion de documents scientifiques de niveau recherche, publiés ou non, émanant des établissements d'enseignement et de recherche français ou étrangers, des laboratoires publics ou privés.

[Click here to view linked References](#)

myjournal manuscript No. (will be inserted by the editor)
--

# Time-dependent methodology for non-stationary mass flow rate measurements in a long micro-tube

## Experimental and numerical analysis at arbitrary rarefaction conditions

Marcos Rojas-Cárdenas<sup>1</sup> · Ernane Silva<sup>2</sup> · Minh-Tuan Ho<sup>3,4</sup>  
César J. Deschamps<sup>2</sup> · Irina Graur<sup>3</sup>

Received: date / Accepted: date

**Abstract** This paper reports the experimental and numerical analysis of time-dependent rarefied gas flows through a long metallic micro-tube. The experimental methodology was conceived on the basis of the constant volume technique and adapted to measure the evolution with time of a transient mass flow rate through a micro-tube. Furthermore, the characteristic time of each experiment, extracted from the pressure measurements in each reservoir, offered a clear indication on the dynamics of the transient flow as a function of the gas molecular mass and its rarefaction level. The measured pressure evolution with time at the inlet and outlet of the micro-tube was compared to numerical results obtained with the BGK linearized kinetic equation model. Finally we present an original methodology to extract stationary mass flow rates by using the tube conductance, which can be associated to the characteristic time of the experiment, measured for different mean pressures between two tanks. The results were obtained

in a wide range of rarefaction conditions for nitrogen ( $N_2$ ). A brief comparison is offered in respect to R134a ( $CH_2FCF_3$ ), too, a heavy polyatomic gas which is typically used in the refrigeration industry.

**Keywords** micro-flows · transient flows · MEMS · gas rarefaction · kinetic theory

## 1 Introduction

Since the advent of micro-electro-mechanical systems (MEMS), the physical investigations performed on gas flows at a microscopic scale have become of great interest for various applications that touch almost every industrial field, such as fluidic microactuators for active control of aerodynamic flows, mass flow and temperature microsensors, micropumps, microsystems for mixing or separation for local gas analysis, mass spectrometers, vacuum applications, pressure gauges, dosing valves and microheat exchangers. In practical applications, these microfluidic devices are often required to function in transient conditions, hence a time-dependent analysis of the flow is needed. To this day not much attention has been dedicated to study and analyze time-dependent gas flows in micro devices, to the extent that experimental data on the matter is basically lacking.

In micro-devices the equivalent mean free path of the gas molecules ( $\ell$ ) can be of the same order as the characteristic dimension ( $L$ ) of these devices. In this case the fluid can be considered to be under rarefied conditions and it cannot be treated as a continuum medium as it usually done by classic fluid mechanics. Depending on their level of rarefaction, which can be characterized by a rarefaction parameter  $\delta = L/\ell$ , micro gas flows often require modeling by means of molecular based

<sup>1</sup>Institut Clément Ader CNRS UMR 5312, Université de Toulouse, INSA-ISAE-Mines Albi-UPS, Toulouse, France.  
E-mail: marcos.rojas@insa-toulouse.fr

<sup>2</sup>Polo Research Laboratories for Emerging Technologies in Cooling and Thermophysics, Federal University of Santa Catarina, 88048-300, Florianópolis SC, Brazil.  
E-mail: ernane@polo.ufsc.br; deschamps@polo.ufsc.br

<sup>3</sup>Aix-Marseille Université, CNRS, IUSTI UMR 7343, 13453, Marseille, France.  
E-mail: irina.martin@univ-amu.fr

<sup>4</sup>James Weir Fluids Laboratory, Department of Mechanical and Aerospace Engineering, University of Strathclyde, Glasgow G1 1XJ, UK.  
E-mail: minh-tuan.ho@strath.ac.uk

approaches. Gas rarefaction induces macroscopic non-equilibrium effects at the interface between gas and solid surfaces for the gas macroscopic parameters, such as viscous and thermal slip and temperature jump at the wall, for the gas velocity and its temperature, respectively. These non-equilibrium phenomena are affected by the specific configuration of the surface of the micro-device, such as surface roughness and materials, and the molecular structure of the gas considered (Sharipov [2011]).

At the current state of the art, experimental observation on rarefied gas flows is generally limited to stationary flow configurations. Particularly, most works aim to measure stationary isothermal mass flow rates as a function of the flow rarefaction in order to identify the magnitude of the velocity slip at the wall. This particular phenomenon has been greatly investigated since the modified boundary conditions to be used together with the Navier-Stokes equations for slightly rarefied gas flows take account of gas slip at the wall. However, these slip boundary conditions require an empirical adjustment which depends on the gas tangential momentum accommodation at the wall [Porodnov et al, 1974; Harley et al, 1995; Arkilic et al, 1997; Ewart et al, 2007; Pitakarnnop et al, 2010; Perrier et al, 2011; Yamaguchi et al, 2011; Silva et al, 2016].

Even if the main focus of attention in rarefied gas flows has been the measurement of stationary flow configurations, some authors have numerically studied transient rarefied gas flows (Colin [2005]; Lihnaropoulos and Valougeorgis [2011]; Sharipov [2012b, 2013]; Vargas et al [2014a]; Sharipov and Graur [2014]). Nevertheless, very little experimental efforts on the topic have been conducted so far. The only experimental study that at our knowledge offers an insight on transient rarefied gas flows is the recent work of Vargas et al [2014b], who measured the pressure difference between inlet and outlet of a single short tube as a function of time for different single gases and binary gas mixtures. The hybrid model they presented could qualitatively but not quantitatively follow the experimental results.

Due to this lack of experimental observation, the primary goal of the present study was to measure the relaxation process of a gas diffusing through a long micro-tube. The relaxation process refers to the pressure variation with time in two tanks, set at the inlet and outlet of a microtube, from an initial pressure difference stage until a final equilibrium stage of pressure equality.

Furthermore, by monitoring the entire relaxation process of pressure evolution inside two tanks of equal volumes at the inlet and outlet of the micro-device, we demonstrated that it is indeed possible to extract an unique conductance value that depends only on the

average pressure of the experiment, the geometry of the channel and the gas nature. This was achieved by means of a dynamic constant volume technique that was firstly proposed to measure thermally driven gas flows by Rojas-Cardenas et al [2011]. The originality in respect to the classic constant volume technique (Arkilic et al [1997], Yamaguchi et al [2011], Ewart et al [2006]) relies on the fact that a dynamic measurement technique considers the time-dependency of pressure during the full duration of the pressure relaxation process obtained from one single experiment. The methodology therefore takes under account the intrinsic non-stationarity of the pressure measurements and profits from it to characterize the relaxation process by a characteristic time that can be associated to the conductance of the channel used.

From these experiments it is not only possible to measure a single conductance value, but it is also possible to associate to the pressure evolution with time the time-dependent mass flow rate along the micro-tube.

The experiments were performed for different initial pressure ratios and for a large spectrum of rarefaction conditions.

Finally, the obtained experimental time-dependent results were compared with the numerical solution of the linearized BGK model kinetic equation in the case of transient flows (Sharipov and Graur [2014]).

The understanding of the phenomena relating the non-equilibrium effects of viscous slip to the transient gas macroscopic displacement in micro-systems under different type of rarefaction conditions and for different gases could be used to develop interesting applications such as for example gas separators or accurate micro mass flow rates regulating devices.

## 2 Experimental Apparatus

The experimental set-up was composed of a single metallic (stainless-steel) micro-tube of circular cross-section, two reservoirs, two capacitance diaphragm pressure gauges, two thermocouples, a vacuum pump and the acquisition system (Figure 1). The single metallic micro-tube ( $L_t = 92.22 \pm 0.01\text{mm}$ ,  $D = 435.5 \pm 3.5\mu\text{m}$ ) was connected to two tanks which were positioned at the inlet and outlet of the capillary.

The volume of the tanks was chosen to be much larger in respect to the volume of the micro-tube. Two sets of inlet/outlet tank volumes were used. The main experimental campaign was performed for a first set of volumes with almost equal dimensions, that is  $V_1 = 173.2 \pm 0.5\text{ml}$  and  $V_2 = 174.5 \pm 0.5\text{ml}$  ( $V_1/V_2 = 0.9926$ ). While the second set of volumes were chosen to be of considerably different dimensions  $V_1 = 181.1 \pm 0.5\text{ml}$

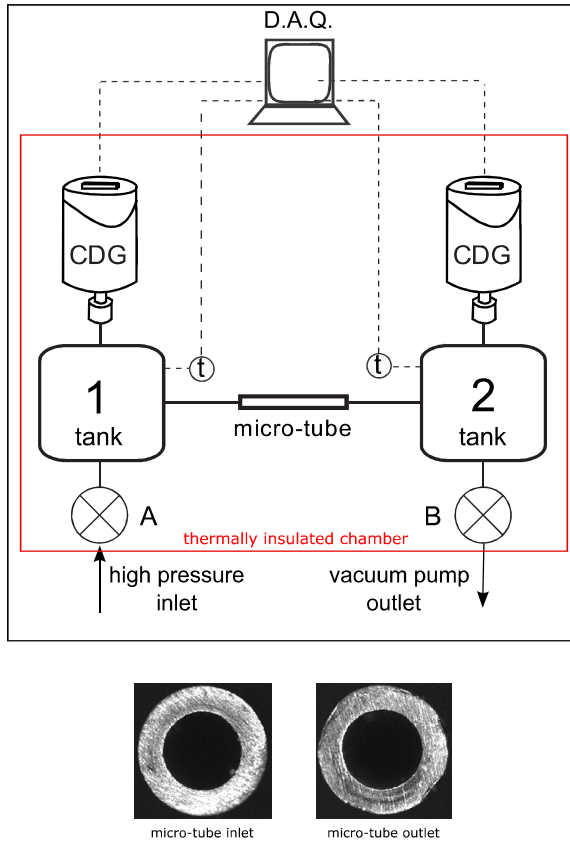


**Fig. 1** Above: The experimental apparatus composed by the micro-tube, two temperature sensors ( $t_1$  and  $t_2$ ), two tanks (R1 and R2) and the INFICON capacitance pressure diaphragm gauges (CDG). Below: Details of the circular cross-section micro-tube.

and  $V_2 = 28.5 \pm 0.1 \text{ ml}$  ( $V_1/V_2 = 6.354$ ). The indexes 1 and 2 stand for inlet and outlet of the tube, respectively. The two tanks were appositely designed to host the single micro-tube. However, the experimental apparatus can be re-arranged in order to host in its test-section a great variety of micro-fluidic devices.

The temperature inside both tanks was continuously monitored by means of two thermocouples and it was stabilized at around  $T_m = 295.5 \pm 0.5 \text{ K}$  during the full duration of one experiment. The apparatus was thermally insulated from the external room by means of the same adiabatic chamber used by Pitakarnnop et al [2010]. Additionally, an efficient isothermal stability was achieved due to the high thermal inertia of the two stainless steel tanks. The temperature oscillations at the inlet and outlet tanks were evidently lower than the sensibility of the temperature sensors, as it can be seen from Figure 2. We estimated these oscillations in the order of  $dT/T_m = 10^{-3}$ .

The inlet tank was connected by means of valve A to high pressure reservoirs containing nitrogen  $N_2$  and

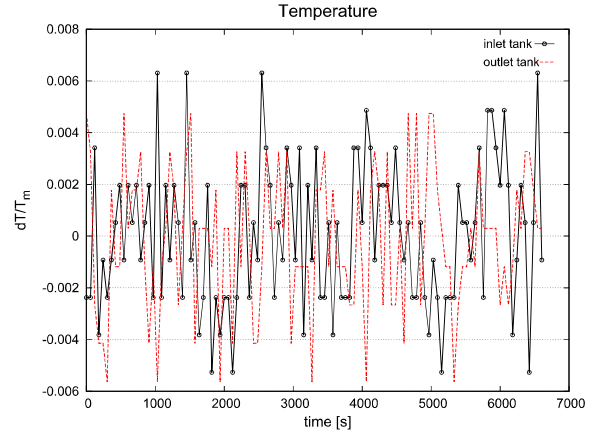


**Fig. 2** Temperature oscillations around the average temperature  $T_m = 295.5 \pm 0.5 \text{ K}$  measured by two temperature sensors ( $t_1$  and  $t_2$ ) at the inlet and outlet tanks (R1 and R2).

R134a ( $CH_2FCF_3$ ), a commonly used refrigerant fluid. The outlet tank was connected by means of valve B to a vacuum pump. The test section could be vacuumed until pressures as low as  $10^{-2} \text{ Pa}$  and it was regulated by means of valve B. The rarefaction conditions imposed in the micro-tube ranged from transition to near hydrodynamic regime.

The fast response capacitance diaphragm gauges (CDG) monitored the pressure variation with time inside the two tanks. The acquisition frequency of the pressure gauges was of  $33 \text{ Hz}$ . CDGs with different full scales were used as a function of the nominal pressure in the system, which allowed us to improve the measurements accuracy at low pressures (see Table 1 for specifications).

### 3 Experimental methodology

In this section we introduce the dynamic constant volume technique which can be used to extract a time-dependent mass flow rate at the inlet or outlet of the micro-device. In order to do this we give a brief description of the well-known classical constant volume technique and present its limitations and how it can be extended into a dynamic constant volume technique. Finally, as a consequence of the new methodology, we present the extraction of the conductance from the exponential relaxation of the pressure variation with time.

#### 3.1 Constant volume technique

From the constant volume technique it is possible to measure the stationary mass flow rate along the tube by correlating the variation of mass inside tanks 1 and 2



F. S. <sup>1</sup> [Pa]	Accuracy % of r. <sup>2</sup>	Resolution % of F.S	Lowest r. % of F.S.	Acq. frequency
13332 } 1333.2 } 133.32 }	0.2	0.003	0.01	33Hz
			<sup>1</sup> full scale	<sup>2</sup> reading

**Table 1** Characteristics of the capacitance pressure gauges CDG025.

to a linear pressure variation with time. Thus, the constant volume technique consists on performing a quasi-stationary macroscopic thermodynamic study inside a defined volume of a tank by means of the ideal gas law

$$p_1 V_1 = M_1 R T, \quad p_2 V_2 = M_2 R T, \quad (1)$$

where  $R$ ,  $T$ ,  $p_i$ ,  $V_i$ , and  $M_i$ , are, respectively, the specific gas constant, the temperature, the pressure, the tank volume and the mass of the gas in the tank. The subscript  $i = 1, 2$  defines the equation in respect to where the measurement was conducted, that is the tank at the inlet or outlet of the microtube. As the experiments were isothermal, the temperature in both tanks was exactly the same.

If one differentiates eq. (1) by considering a constant tank volume, it is possible to write for tank 2

$$dM_2 = \frac{V_2}{RT} dp_2 \left( 1 - \frac{dT/T}{dp_2/p_2} \right), \quad (2)$$

while an analogous expression can be written for the other tank.

If the relative temperature variation in the tank can be considered as negligible in relation to the relative pressure variation and by defining a specific time interval,  $dt$ , it is then possible to obtain the isothermal mass-flow-rate  $\dot{M}_2$  from eq.(2) as

$$\dot{M}_2 = \frac{V_2}{RT} \frac{dp_2}{dt}, \quad \epsilon = \frac{dT/T}{dp_2/p_2} \ll 1. \quad (3)$$

Since here the variation of the thermodynamic parameters  $dM$  and  $dp$  are sufficiently small, one can approximate  $dM/dt$  and  $dp/dt$  as the time derivative of the mass, *i.e.* mass flow rate  $\dot{M}$ , and the time derivative of pressure, respectively. For each experiment the oscillations of temperature were in the order of  $dT/T = 10^{-3}$  and the variation of pressure in average was in the order of  $dp/p = 10^{-1}$ . Therefore the  $\epsilon$  parameter as defined in eq. (3) was estimated to be negligible ( $\epsilon \approx 0.01$ ).

From the mass conservation law the mass flow rate leaving the first tank is necessarily equal to the mass flow

rate entering into the second tank and it is therefore possible to write

$$\dot{M}_2 = -\dot{M}_1 = \dot{M}. \quad (4)$$

Consequently, from eqs. (3) and (4), one can simply notice that by subtracting

$$\frac{dp_1}{dt} - \frac{dp_2}{dt} = RT \left( \frac{\dot{M}_1}{V_1} - \frac{\dot{M}_2}{V_2} \right), \quad (5)$$

it is possible to deduce the dependence of the mass variation in one tank to the pressure difference variation between both tanks, as

$$\dot{M} = -\frac{V_0}{RT} \frac{d(\Delta p(t))}{dt}, \quad V_0 = \frac{V_1 V_2}{V_1 + V_2}, \quad (6)$$

where  $\Delta p(t)$  is the pressure difference between the two reservoirs:  $\Delta p(t) = p_1(t) - p_2(t)$ .

In the classical constant volume technique case the duration of the time interval  $dt$  is notably chosen to be small enough in order to respect the tank stationary assumption in both reservoirs, that means that the variation of any macroscopic quantity inside the tanks needs to be negligible. However, this time interval needs to be long enough, too, since the pressure changes in both tanks must be measured within an acceptable accuracy. The stationary flow assumption physically justifies that the pressure varies with time in a linear manner and by thus it may be represented with a simple linear least-square fit. Conversely, the measurements consistent with the linear profile justify the stationarity assumptions [Ewart et al, 2006].

### 3.1.1 Limits and extension of the constant volume technique

The first limit of the classical constant volume technique results from the fact that the method does not provide direct access to a real time dependent flow regime. In fact, the method could only be used at a fixed time during one experiment, allowing us to derive various stationary mass flow-rates related to various quasi-stationary states.

Now considering precisely the use of the methodology at a fixed time, some limits can be found considering the two opposite purposes of the technique. A time interval  $dt$  is to be defined where the pressure measurement has to be made. As previously discussed, this time interval must be sufficiently small to allow us to identify the left-hand-side expression of eq.(3) to the time derivative of the mass, namely, to the mass flow rate at a fixed time  $t^*$ , in other words to a mass flow rate considered as stationary. But, nevertheless, it is necessary to

consider a time interval  $dt$ , sufficiently long, that allows us to extract a pressure variation measurement that has a substantial physical meaning.

Thus, in some cases, where a very fast pressure variation with time is initially induced, it may be difficult to completely verify both the previously defined constraints: in such cases the error on the stationary mass flow rate evaluation would be without any doubt increased. As previously discussed, when the pressure varies with time in a linear way, this error becomes, by all matters, completely negligible.

### 3.2 Dynamic constant volume technique

The technique proposed herein is not limited to a quasi-stationary approach, *i.e.* to the measurement of a linear pressure variation with time.

Firstly, this dynamic method allows us to obtain, through the pressure time-derivative, an explicit expression of the time-depending mass flow rate. Therefore, regarding the stationary mass flow rate evaluation, the new methodology eliminates the necessity of using a time interval, where the pressure varies linearly, but uses the whole process of the pressure decay in both reservoirs. Secondly, this methodology offers new interesting possibilities, since the pressure difference decay with time between both reservoirs can be associated to a conductance value which depends only on the tube geometry, the gas used and the average pressure in the micro-device.

#### 3.2.1 Pressure variation with time

In order to obtain a pressure variation with time in both reservoirs, an initial pressure difference,  $\Delta p_0$ , is imposed between the two tanks. Thereafter, since the tanks are connected only by the micro-tube (valve A and B are closed, see Fig. 1), the pressure inside the two tanks can relax to a final state of equilibrium, *i.e.* to a final pressure equality stage where  $p_f = p_1(t_f) = p_2(t_f)$ .

For every experiment we monitored the whole pressure relaxation process by means of two capacitance diaphragm gauges connected to the tanks. For convenience, we always imposed a higher initial pressure in tank 1 in respect to tank 2, that is  $p_1(t) > p_2(t)$  (Figure 3).

The relation between the pressure variations in both tanks, that is from the initial pressure  $p_i(t_0)$  imposed to the final pressure  $p_f$  reached, can be computed a priori as this variation closely relates to the tanks volume ratio. From the ideal gas law, admitting again the mass conservation along the micro tube at any time, see eq. (4), one can write the following relation for the two

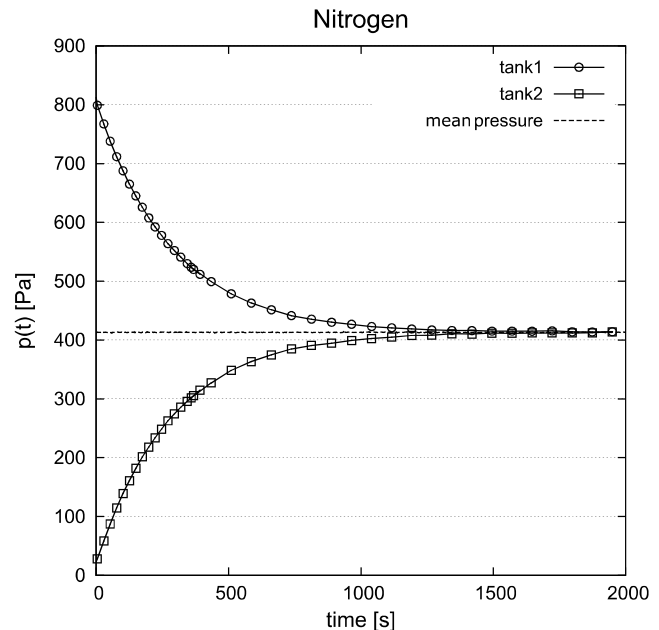


**Fig. 3** An initial pressure difference ( $\Delta p_0$ ) is imposed between the two reservoirs that leads to a pressure relaxation with time in the two tanks 1 and 2 until a final pressure equilibrium is reached  $p_f = p_1(t_f) = p_2(t_f)$ . The initial pressures are  $p_1(t_0) = 805.7 Pa$ ,  $p_2(t_0) = 23.5 Pa$ , the mean pressure varies from  $p_m(t_0) = 414.6 Pa$  to  $p_f = 413 Pa$ . A small fraction of the acquired experimental points are shown for sake of a proper visual representation. The acquisition frequency for each experiment was 33Hz.

tanks if they are maintained at the same temperature  $V_2 dp_2 = -V_1 dp_1$ . This expression can be rewritten in the following form

$$\frac{p_f - p_2(t)}{p_1(t) - p_f} = \frac{V_1}{V_2}. \quad (7)$$

It is clear from Eq.(7) that by adjusting the tanks' volume ratio one could control the pressure variation between initial and final stages. Therefore, from eq. (7) it is possible to estimate the maximal variation of the mean pressure  $p_m = 0.5(p_1 + p_2)$  with time during one experiment between the initial mean pressure  $p_m(t_0) = p_m$  to the final mean pressure  $p_m(t_f) = p_f$

$$\frac{p_f}{p_m(t_0)} = \frac{2(1 + k_V k_p)}{(1 + k_V)(1 + k_p)}. \quad (8)$$

In previous expression  $k_p = p_1(t_0)/p_2(t_0)$  is the initial pressure ratio,  $k_V = V_1/V_2$  is the volume ratio. As it is clear from Eq. (8), when the tank volumes are equal  $k_V = 1$ , the mean pressure  $p_m(t)$  does not vary in time, *i.e.*  $p_m(t) = p_f$  during the whole experiment.

By using Eq. (8) one can estimate the maximal amplitude of mean pressure variation between its initial state  $p_m(t_0)$  and its final state  $p_f$  for a known tank volumes ratio and initial pressure ratio. For example for

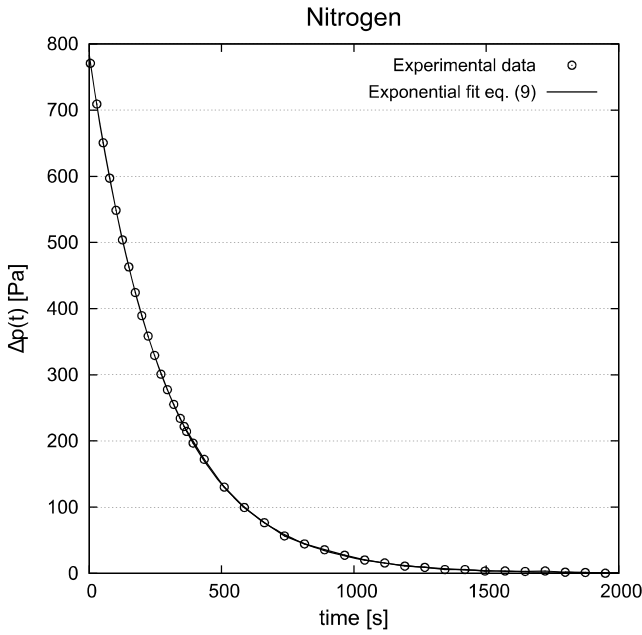


**Fig. 4** Pressure difference variation with time  $\Delta p(t)$ : an initial pressure difference is imposed at the inlet and outlet of the tube, this engenders a pressure relaxation in the two tanks 1 and 2 until a final pressure equilibrium is reached  $\Delta p(t_f) = 0$ . The experimental results were fitted by eq. (13). The mean pressure is  $413 Pa$ . A small fraction of the acquired experimental points are shown for sake of a proper visual representation. The acquisition frequency for each experiment was 33Hz.

the case shown in Figure (3) where  $V_1/V_2 = 0.9926$ ,  $p_1(t_0) = 805.7 Pa$  and  $p_2(t_0) = 23.5 Pa$  the mean pressure varies from  $p_m(t_0) = 414.6 Pa$  to  $p_f = 413 Pa$ , that means  $\approx 0.35\%$ . This information will be crucial for what concerns the conductance determination performed in the following section.

### 3.2.2 Exponential relaxation with time

By analogy to Ohm's law one can relate the pressure difference ( $p_1 - p_2$ ) across the micro-tube to the "potential", the flow throughput  $\dot{Q}$  to the "current" and the conductance  $C$  to the inverse of the "an electrical resistance". Therefore, one can define the conductance of the tube as

$$C = -\frac{\dot{Q}_1}{p_1 - p_2}, \quad C = \frac{\dot{Q}_2}{p_1 - p_2}, \quad (9)$$

where  $C$  is the same for both reservoirs, admitting the mass conservation of the flow along the micro-tube [Arkilic et al, 2001]. The flow throughput  $\dot{Q}$ , commonly used in the field of vacuum science and technology to express gas flow rates [Jousten, 2008], is defined as

$$\dot{Q}_i = \frac{d(pV)_i}{dt} = RT\dot{M}_i, \quad (10)$$

and, as seen above, it can be easily correlated to the mass flow rate by using eq. (3). We can now relate the conductance  $C$  in eqs. (9) to the pressure variation in time in each reservoir by means of eq. (10) in the following form:

$$\frac{dp_1}{dt} = -\frac{C}{V_1}(p_1 - p_2), \quad \frac{dp_2}{dt} = \frac{C}{V_2}(p_1 - p_2), \quad (11)$$

where  $V_1$  and  $V_2$  are constant tank volumes. By subtracting one of the previous equations to the other, we can obtain a differential equation for the pressure difference  $\Delta p(t)$  between the tanks:

$$\frac{d(\Delta p(t))}{\Delta p(t)} = -\frac{C}{V_0} dt. \quad (12)$$

This differential equation can be easily solved if the constancy of the conductance  $C$  in time is assumed, then the solution of Eq. (12) has the form

$$\Delta p(t) = \Delta p_0 \exp\left(-\frac{t}{\tau}\right), \quad \tau = \frac{V_0}{C}, \quad (13)$$

where  $\Delta p_0$  is the initial pressure difference at  $t = 0$  and  $\tau$  is the characteristic time of the experiment or the system relaxation time.

The pressure difference variation with time between tank 1 and 2 can be thus associated to an exponential decay for the case where the conductance of the tube is constant during one single experiment. In addition we can note that  $\tau$  can be extracted from the experimental pressure variation with time (Figure 4). This value of the characteristic time allows us to obtain the tube conductance corresponding to the mean pressure of an experiment.

### 3.2.3 Time dependent and steady state mass flow rate measurements

In the previous section we derived the exponential expression of the pressure difference variation with time. By using eqs. (6) and (13) we can now express the mass flow rate variation with time using the analytical derivation of the pressure difference variation with time. Therefore, for the case of isothermal tanks the mass flow rate entering in tank 2 can be written as

$$\dot{M}_2(t) = \frac{V_0}{RT} \frac{\Delta p_0}{\tau} \exp\left(-\frac{t}{\tau}\right). \quad (14)$$

This expression of the mass flow rate, eq. (14), can be used in two different ways:

- The mass flow rate depends on time, but for a given time  $t = t^*$  this mass flow rate can be identified as the stationary mass flow rate corresponding to the pressure difference between the extremities of the tube, i.e.  $p_1(t^*) - p_2(t^*)$ .

- It is possible to directly consider the transient mass flow rate  $\dot{M}(t)$  through the tube for the full duration of one experiment in order to study the transient phenomenon.

### 3.2.4 On the conductance constancy condition

As it was shown in Section 3.2.2, the expression of the pressure difference variation with time [eq. (13)] and, therefore, the expression of the mass flow rate variation with time [eq. (14)], are valid under the assumption of having a constant conductance  $C$  during one single experiment. Let us now analyze for which conditions the conductance constancy assumption is thus satisfied. As seen in Section 3.2.2 the conductance can be easily related to the mass flow rate along the tube leaving the first reservoir or entering the second reservoir. For the case of tank 2, one can write

$$C = \frac{\dot{M}RT}{p_1 - p_2}. \quad (15)$$

It is known that the mass flow rate  $\dot{M}$  imposed by a pressure difference  $p_1 - p_2$  flowing through a long tube of diameter  $D \ll L$  can be related to the dimensionless mass flow rate  $G$  as

$$\dot{M} = G \frac{\pi D^3 (p_1 - p_2)}{8vL}, \quad (16)$$

where  $v = \sqrt{2RT}$  is the most probable molecular speed [Sharipov, 1997]. Comparing Eqs. (15) and (16) one can easily conclude for an isothermal configuration that the conductance is constant when the dimensionless mass flow rate  $G$  is constant. Since  $G$  is only a function of the rarefaction parameter [Sharipov, 1997], it is possible to state that if the gas rarefaction is constant, the conductance is constant, too. The mean rarefaction parameter along the tube can be defined as

$$\delta_m = \frac{p_m D}{\mu(T)v}, \quad (17)$$

where  $\mu(T)$  is the gas viscosity which depends only on temperature. The values of  $G$  are provided in Sharipov [1997] for a large range of the rarefaction parameter. It becomes clear from eq. (17) that for an isothermal case, the rarefaction parameter  $\delta_m$  depends only on pressure. Therefore, when the mean pressure does not vary during the experiment the dimensionless mass flow rate  $G$  is constant and hence the tube conductance remains constant too. If the rarefaction varies greatly along the channel for large pressure ratios imposed, the dimensionless mass flow rate varies along the channel, too, nevertheless it has been proven that when the pressure ratio is  $p_1/p_2 = 4$  the dimensionless mass flow rate  $G$

can be approximated with a 5% accuracy from the value calculated by means of the mean pressure between the inlet and outlet tank, i.e.  $G(\delta_m)$  [Sharipov, 1997; Graur and Sharipov, 2008]. As it was shown in Section 3.2.1 the mean pressure does not vary during an experiment when the inlet/outlet volumes are identical. Therefore it is interesting to have an estimation of the variation of dimensionless mass flow rate  $G$ , and consequently of the conductance  $C$ , as a function of the rarefaction parameter defined by the mean pressure. An expression of the dimensionless mass flow rate  $G$  as a function of the mean rarefaction parameter  $\delta_m$  was proposed in Sharipov et al [2010] for the case of complete accommodation of molecules to the wall:

$$G(\delta_m) = \frac{8}{3\sqrt{\pi}} \frac{1 + 0.025 \delta_m^{0.7} \ln\left(\frac{\delta_m}{2}\right)}{1 + 0.448 \delta_m^{0.8}} + \left(\frac{\delta_m}{8} + 1.018\right) \frac{\delta_m}{2 + \delta_m}. \quad (18)$$

By analyzing eq. (18) one can see that for small deltas ( $\delta_m \rightarrow 0$ , low pressures) the dimensionless mass flow rate tends to a limit value  $G(\delta_m) \rightarrow \frac{8}{3\sqrt{\pi}}$ , however for ( $\delta_m \rightarrow \infty$ )  $G(\delta_m)$  becomes linearly proportional to  $\delta_m$  tending to the hydrodynamic limit, where the mass flow rate is defined by the Poiseuille solution, that is  $G(\delta_m) = \delta/8$ .

Since the dimensionless mass flow rate is correlated to the mass flow rate and the conductance from eqs. (15) and (16)

$$C = \frac{\pi D^3 v}{16L} G, \quad (19)$$

by using eq. (18) one can obtain two limit values for the conductance, one in the free molecular flow

$$C^{FM} = \frac{\sqrt{\pi} D^3 v}{6L} \quad (\delta_m \rightarrow 0), \quad (20)$$

and one in the hydrodynamic flow, which coincides with the Poiseuille solution and is linearly proportional to the mean pressure

$$C^H = \frac{\pi D^3 v}{128L} \delta_m \quad (\delta_m > 10^3). \quad (21)$$

Therefore, it is clear that the limit case of hydrodynamic flow could be sensitive to conductance variations during the duration of one experiment, specially for cases above  $\delta_m > 10$ , where the influence of the mean pressure starts to be relevant. It was thus of great importance to chose an upper limit value of mean pressure variation with time in respect to the initial pressure ratio imposed at the beginning of one experiment. Since the reservoirs' volume ratio is known, we can establish

a condition on the maximum pressure ratio  $k_p$  to be imposed to have a maximum mean pressure variation with time  $p_f/p_m$  of the order of 1%. From eq. (8), for the first case configuration of volume ratio  $V_1/V_2 = 0.9926$  an initial pressure ratio  $k_p = 33.75$  relates to a maximum mean pressure variation of 0.35%, therefore, one can consider that this volume ratio configuration does not generate any mean pressure variation during the whole duration of one experiment. For the second case configuration of volume ratio  $V_1/V_2 = 6.354$  an initial pressure ratio  $k_p = 1.1475$  relates to a maximum mean pressure variation of 5%, therefore, eq. (13) can be applied to this case configuration only for relatively short relaxation experiments. Since the conductance  $C$  in the worst case scenario is linearly proportional to  $p_m$ , we can state that in our experiments we have chosen to work with a maximum of 1% uncertainty value related to the measurement methodology on  $C$ .

### 3.2.5 Mass flow rate measurements uncertainty

To estimate the measurement uncertainty when using the dynamic constant technique we can rewrite eq. (14) in the following form

$$\dot{M}(t) = \frac{C}{RT} \Delta p_0 \exp\left(-\frac{C}{V_0} t\right). \quad (22)$$

Using the classical technique to calculate the mass flow rate measurements uncertainty if one measures it using Eq. (22).

$$\frac{d\dot{M}}{\dot{M}} = \frac{dC}{C} + \frac{d(\Delta p)}{\Delta p} + \frac{dV_0}{V_0} + \frac{d\epsilon}{\epsilon}. \quad (23)$$

The first term is related to the constancy of the conductance and the fitting coefficient  $\tau$  and can be estimated at around  $\frac{dC}{C} = 1\%$ , the second uncertainty can be related to pressure sensors used  $\frac{d(\Delta p)}{\Delta p} = 0.5\%$ , the third term is related to the volume measurement uncertainty which was estimated to be around  $\frac{dV_0}{V_0} = 0.5\%$ , while the last term is related to the relative temperature variation effects, see Section 3.1 for details, and it is estimated to be of the order of  $\frac{d\epsilon}{\epsilon} = 1\%$ .

## 4 Experimental Results

### 4.1 Pressure variation with time

The pressure variation with time experiments gave a clear idea on which parameters affect the relaxation process from the initial non-equilibrium stage and the final equilibrium stage of pressure equality. It was possible to identify some main parameters that affected

Gas	Molecule	$\mu \times 10^{-5} [Pa \cdot s]$	R [ $Jkg^{-1}K^{-1}$ ]
Nitrogen	$N_2$	1.775	297
R134a	$CH_2FCF_3$	1.181	81.5

**Table 2** Gas properties

the process, such as the gas used, the mean rarefaction of the gas ( $\delta_m$ ), the tanks dimensions ( $V_1, V_2$ ) and the tube conductance ( $D, L$ ). By keeping the tube geometry as a constant parameter, we were able to extract the influence of the gas rarefaction, the gas molecular composition and the tanks volumes over the pressure variation with time behavior.

It is possible to characterize a single experiment by defining its initial pressure difference  $\Delta p_0$  and its initial state of mean rarefaction as a function of the rarefaction parameter  $\delta_m$ . The values of the gas viscosity and specific gas constant are given in Table 2.

The pressure variation with time changes radically as a function of the gas rarefaction, *i.e.* mean rarefaction parameter  $\delta_m$ , see Fig. 5 left. For the same initial pressure difference ( $\Delta p_0$ ) imposed, but for different  $\delta_m$ , the pressure variation with time is much slower for rarefied flows that tend to the free molecular regime ( $\delta_m = 0.5$ ) in respect to flows in near hydrodynamic regime ( $\delta_m = 338$ ). For example, the time that a flow of nitrogen needs to reach its final state of equilibrium is around  $t_f = 200s$  for  $\delta_m = 338$  (near hydrodynamic regime), around  $t_f = 1500s$  for  $\delta_m = 19.5$  (slip regime) and around  $t_f = 4000s$  for  $\delta_m = 0.5$  (transition regime). Furthermore, the pressure variation with time is greatly influenced by the molecular weight of the gas (Fig. 5 right). For same initial rarefaction conditions, same initial pressure difference and same tank volumes ( $V_1/V_2 = 6.35$ ;  $V_0 = 24.62ml$ ), a heavier gas is always slower to reach its final state of equilibrium than a lighter gas. For example, a nitrogen flow needs around 600s to reach its final equilibrium stage against approximately 1000s for R134a at same rarefaction conditions,  $\delta_m = 16.4$ , which corresponds to slip regime (see Table 2 for the gas properties).

Finally, again an interesting information can be deduced from Figure (5 right). For the pressure variation with time of nitrogen, in respect to different tank volumes used (case 1:  $V_0 = 86.92ml$  and  $V_1/V_2 = 0.9926$  and case 2:  $V_0 = 24.62ml$  and  $V_1/V_2 = 6.354$ ), it is possible to observe that the relaxation process is always slower if the  $V_0$  parameter increases or, in other words,

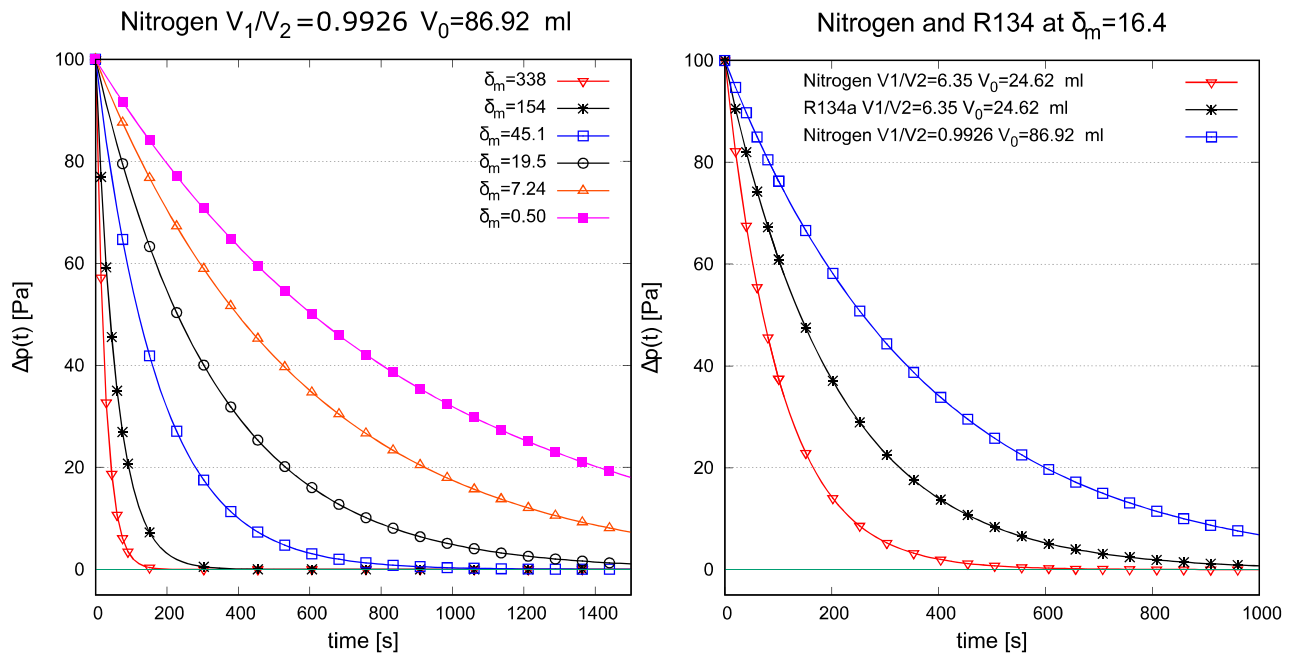


**Fig. 5** Pressure difference variation with time until a pressure equilibrium equality is reached for the same initial pressure difference  $\Delta p_0 = 100 Pa$ . The experimental results are shown for the same initial pressure difference. Left: pressure variation with time of nitrogen at different rarefaction conditions ( $V_1/V_2 = 0.9926$   $V_0 = 86.92 ml$ ). Right: pressure variation with time at the same rarefaction conditions of nitrogen and R134a ( $V_1/V_2 = 6.35$   $V_0 = 24.62 ml$ ). On the right we compare the pressure variation with time for different tank volumes used, too.

if the harmonic mean volume of the two tanks  $V_0$  is increased.

#### 4.2 Conductance

We were able to extract the conductance of the tube at arbitrary rarefaction conditions, from transition to near hydrodynamic regime, by fitting the pressure variation with time [eq. (13)], at different mean pressures. For the same tube and volumes of the tanks, we observed, as expected, that the conductance was strongly influenced by the rarefaction conditions of the flow. For the reasons explained in Section 3.2.4, the here presented conductance results were obtained only for the equal volumes configuration,  $V_1/V_2 = 0.9926$ .

We compared our conductance experimental results to numerical results of the dimensionless mass flow rate  $G$ , obtained by Graur and Sharipov [2008] with the BGK model kinetic equation and to the empirical fit of  $G$ , obtained by Sharipov et al [2010], eq. (18), that reproduces very accurately the BGK solution. Equation (19) is used to relate the two quantities.

It is possible to observe from Figure 6 the very good agreement between the experimentally obtained tube conductance and the results derived from the the solution of the BGK equation. It should be underlined that

the experimental uncertainty on the conductance is related to the uncertainty on the pressure and volume measurements, see eq. (13), as well as to the dimensional quality of the volumes  $V_1$  and  $V_2$  which have to be perfectly identical to assure the constancy of the mean pressure during one experiment. As expected, the experimental results tend towards the free molecular limit for  $\delta_m \rightarrow 0$  [eq. (20)] and the hydrodynamic limit for  $\delta_m > 10^3$  [eq. (21)].

It should be noted that when a comparison between the experimental and numerical results of conductance is carried out, additional sources of experimental errors have to be considered. These sources are related to the tube dimensions measurement and, especially, of the tube diameter, since it intervenes at the power 3 when the numerical values of the dimensionless mass flow rate  $G$  are compared to the experimental values of the conductance  $C$  via eq. (19). Nevertheless, for the case shown on Figure 6, the mean relative deviation between experimental and numerical results is of the order of 1.3%.

#### 4.3 Mass flow rate variation with time

By fitting the data for pressure variation with time results by means of the exponential function of eq. (13)



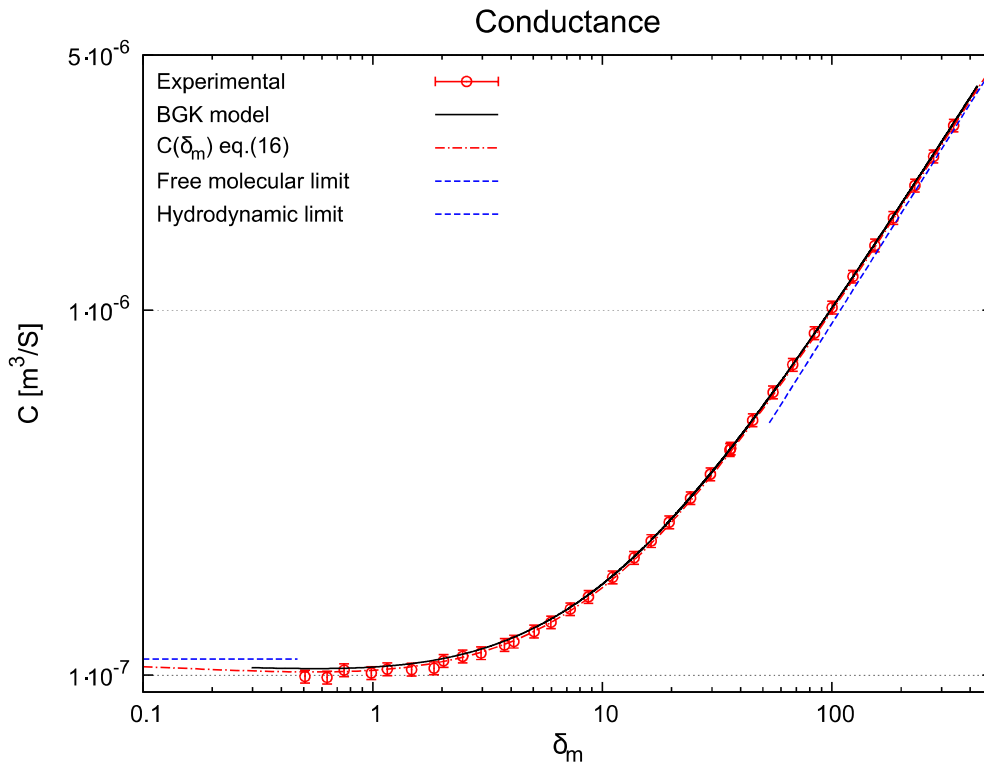


**Fig. 6** Conductance ( $C = V_0/\tau$ ) for nitrogen ( $N_2$ ) as a function of the mean gas rarefaction conditions, that is from transition to near hydrodynamic regime. A comparison is done with values obtained from the BGK kinetic model equation [Graur and Sharipov, 2008] and a fitting equation (eq. 18) [Sharipov et al, 2010]. In the plot also the free molecular (left) and hydrodynamic (right) analytical solutions (eqs. 20, 21) are represented.

and consequently by using eq. (14), the dynamic constant volume technique allowed us to measure non stationary mass flow rates along the full duration of one experiment, that is from the initial pressure difference imposed, where the mass flow rate along the tube was at its maximum, until a final pressure equality equilibrium stage was reached, where the mass flow rate was zero.

It is possible to notice that the influence of the rarefaction on the flow is predominant in the mass flow rate evolution when different rarefaction conditions are compared whereas keeping the same gas and same initial pressure difference imposed (Fig. 7 left). At rarefaction conditions tending to hydrodynamic flow regime, for example at  $\delta_m = 338$ , the initial pressure difference imposed engendered a greater initial mass flow rate, and its final equilibrium state to be reached more rapidly its final equilibrium stage in respect to a higher rarefied flow, for example at  $\delta_m = 0.50$  in transition regime.

The influence of the gas used on the mass flow rate variation with time is also evident, where is always the heavier gas that gives rise to a greater mass flow rate at same rarefaction conditions for same initial pressure differences imposed (Fig. 7 right).

In respect to different tank volumes used for the experiments (case 1:  $V_0 = 86.92ml$  and  $V_1/V_2 = 0.9926$  and case 2:  $V_0 = 24.62ml$  and  $V_1/V_2 = 6.354$ ), it is possible to observe that the mass flow rate variation with time process is slower if the  $V_0$  parameter increases or, in other words, if the total volume of the two tanks increases (Fig. 7 right). This is an analogous consideration in respect to the pressure variation with time section, but for the here shown results it is possible to observe the great reproducibility of the experiments performed: for two completely different experimental campaigns, that is for same tube but different tank volumes used, for the same mean pressure and same initial difference of pressure, the methodology measures the same initial mass flow rates within the experimental uncertainty. For the second case configuration  $V_1/V_2 = 6.354$  the here shown pressure relaxation with time from  $\Delta p_0 = 10Pa$  and  $p_1/p_2 = 1.036$ , corresponds to a mean pressure variation with time of 1.3% and a Conductance variation of 0.7% [eq. (18) and (19)].

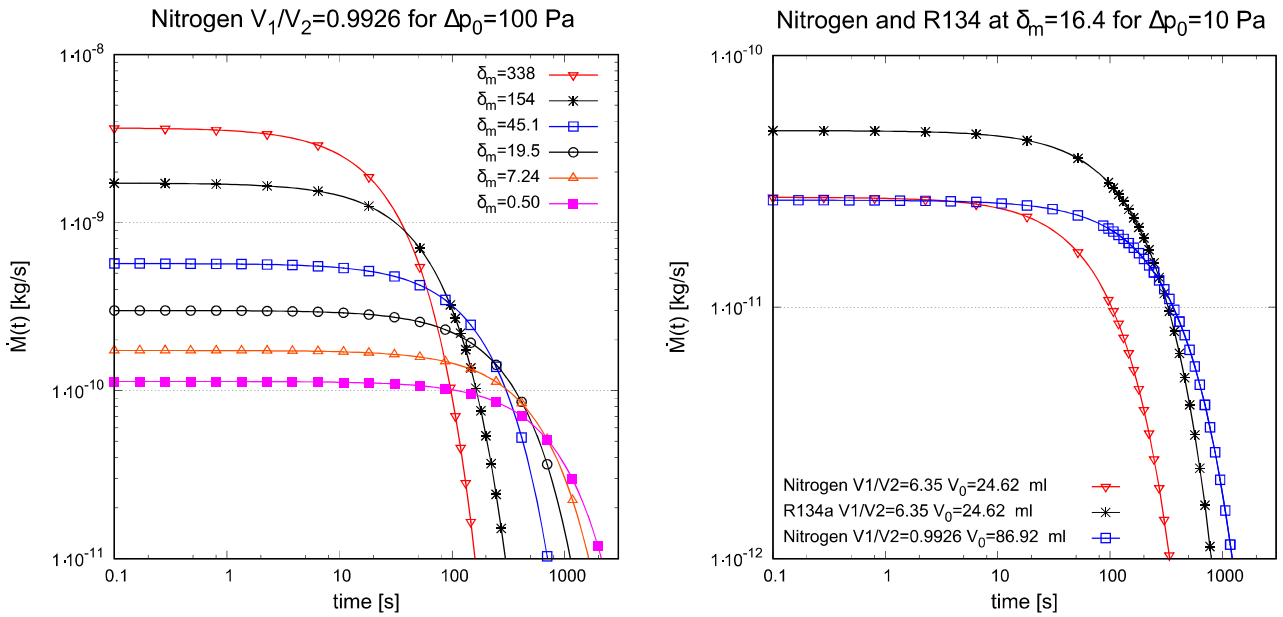


**Fig. 7** Mass flow rate variation with time until a final equilibrium of no motion is reached through the tube for the same initial pressure difference. Left: mass flow rate variation with time of nitrogen at different rarefaction conditions for  $\Delta p_0 = 100 Pa$  (first case configuration:  $V_1/V_2 = 0.9926$  and  $V_0 = 86.92 ml$ ). Right: mass flow rate variation with time at the same rarefaction conditions of nitrogen and R134a for  $\Delta p_0 = 10 Pa$ . Additionally, two volume case configurations were studied (first:  $V_1/V_2 = 0.9926$ ,  $V_0 = 86.92 ml$  and second:  $V_2/V_1 = 6.354$   $V_0 = 24.62 ml$ ).

## 5 Comparison between numerical and experimental results

### 5.1 Pressure variation with time

The experimental pressure variation with time of nitrogen has been compared with numerical results based on the linearized BGK model kinetic equation. The particularity of the numerical results presented here relates to the application of stationary mass flow rate results previously obtained by solving the linearized stationary kinetic equation (Graur and Sharipov [2008]) in order to describe a transient rarefied gas flow (Sharipov and Graur [2014]). This approach is of undeniable efficiency since the computational time required to describe a transient phenomenon is not as significant in respect to a direct solution of the full time-dependent kinetic equation. The deviation between the results obtained by the BGK model and those of the Boltzmann equation does not exceed 5% for the isothermal flows [Sharipov, 2012a]

The results presented in Figure 8 take under account the pressure variation with time of nitrogen inside both the inlet and outlet tanks for two cases (case 1:  $V_0 = 86.92 ml$  and  $V_1/V_2 = 0.9926$  and case 2:  $V_0 = 24.62 ml$  and  $V_1/V_2 = 6.354$ ). Three different rarefaction conditions have been chosen for the comparison at slip, transition, and close to free molecular regime condi-

tions. It is possible to observe that the numerical results for the six cases studied, that is from slip to close to free molecular regime, match very well the experimental results. The small difference that is to be found between numerical and experimental can be due to the uncertainties related to the pressure sensors, the volume dimensions and the diameter measurement. It is to be reminded that the pressure sensors are less accurate for low pressure readings. From the analysis of the deviation between experimental and numerical results (Figure 9), one can clearly see that the deviation is higher for pressure measurements performed at nominal pressures around the reading limit of the CDG (low pressures). Nevertheless, even for low pressure measurements, the deviation between numerical and experimental is always lower than 4%. In the pressure regions where the CDG sensors are more accurate, that is for higher pressures at the inlet tank (upstream), the deviation is always lower than 0.5%, at exception of the measurements performed at  $\delta_m = 0.63$  where the deviation is slightly higher. Let us notice that the different volume size configuration gives always rise to the higher deviation between experimental and numerical. For this case the downstream measurements are not only carried out at the limits of the CDGs sensibility but also the pressure variation with time is much faster in respect to the same volume size configuration, possibly adding up in measurement uncertainties. This remark can be

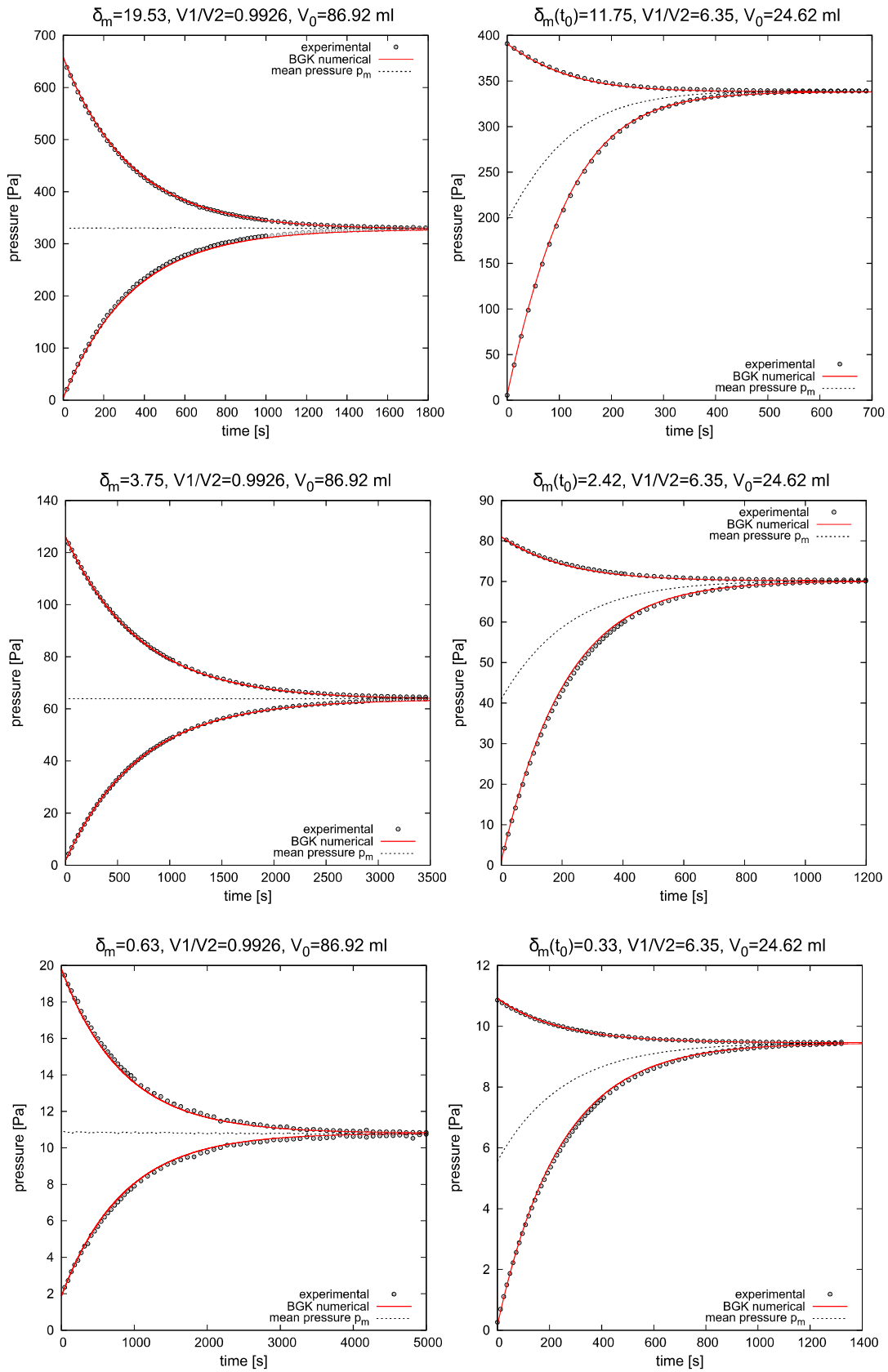


**Fig. 8** Comparison between numerical and experimental results of the pressure variation with time in the inlet and outlet tanks. All comparisons were performed for nitrogen at different mean rarefaction conditions. Left column: first case configuration  $V_0 = 86.92$  ml and  $V_1/V_2 = 0.9926$ . Right column: case 2  $V_0 = 24.62$  ml and  $V_1/V_2 = 6.354$ .

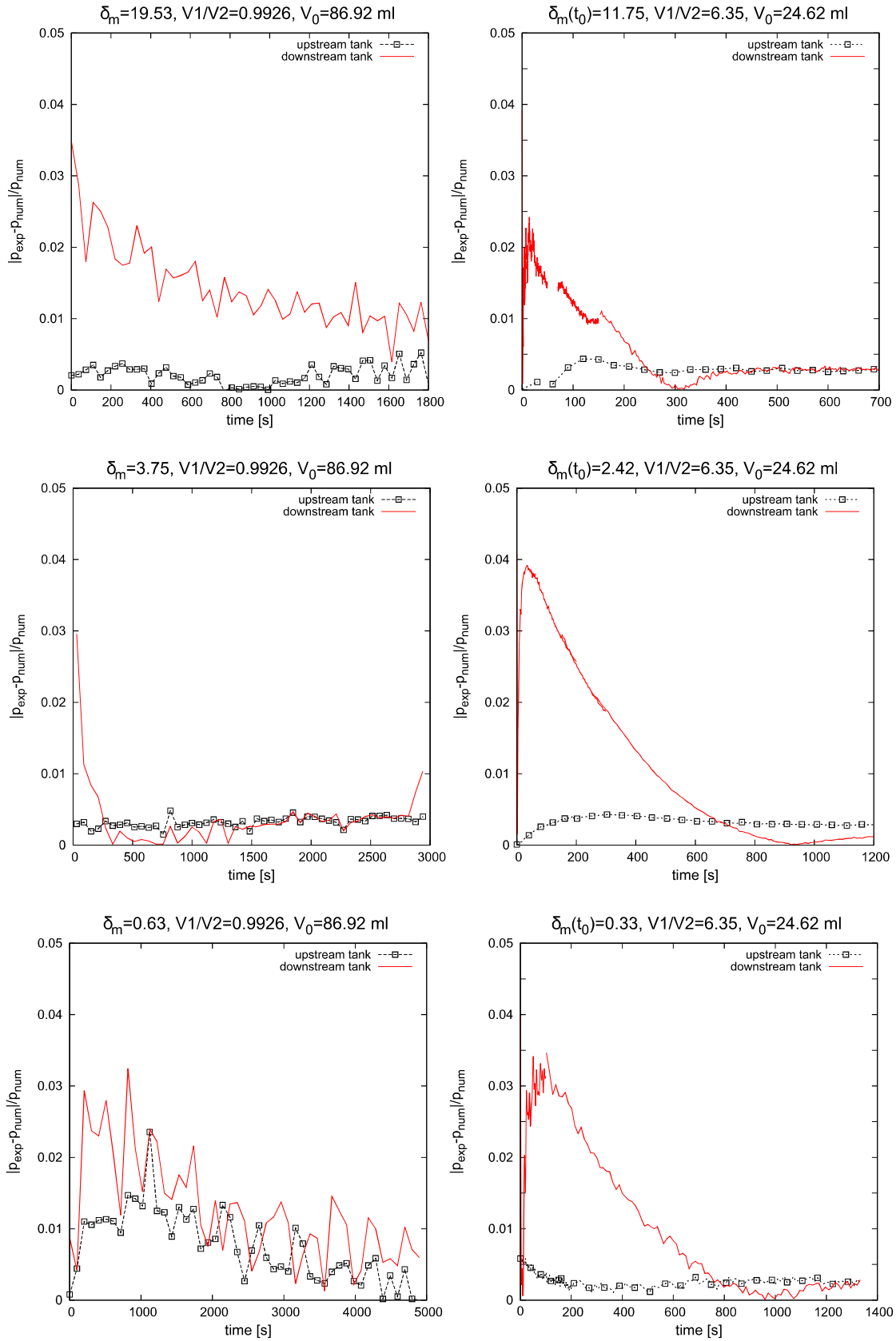


**Fig. 9** Deviation of experimental results in respect to numerical results for the pressure variation with time in the inlet (upstream) and outlet (downstream) tanks. All comparisons were performed for nitrogen at different mean rarefaction conditions. Left column: first case configuration  $V_0 = 86.92 \text{ ml}$  and  $V_1/V_2 = 0.9926$ . Right column: case 2  $V_0 = 24.62 \text{ ml}$  and  $V_1/V_2 = 6.354$ .

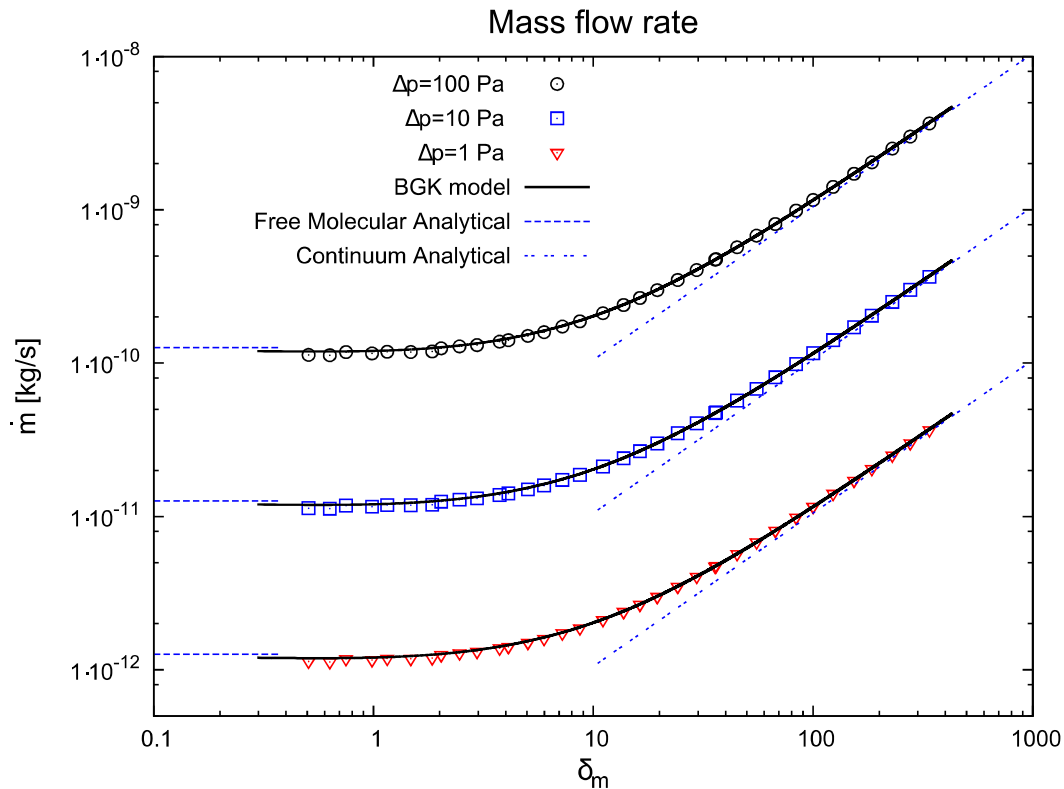


**Fig. 10** Comparison between numerical and experimental results of stationary mass flow rates as a function of rarefaction for several pressure differences imposed for nitrogen. The uncertainties associated to the measurement are smaller than the size of the points ( $\Delta\dot{M}/\dot{M} = 3\%$ )

confirmed by comparing the deviations of  $\delta_m = 0.63$  and  $\delta_m = 0.33$  for the inlet tank case: the deviation is lower for the different volume size configuration since the pressure variation with time speed in this scenario is lower in respect to the same volume size case, even if the nominal pressures of both experiments are comparable. In addition, the pressure variation with time is highly influenced by the volume ratio between the two tanks, therefore, an additional source of uncertainty is introduced by the measurement of the tanks volume ratio, which can be particularly delicate when the ratio between both volumes is high. Nevertheless, let us remind the reader that the pressure variation with time results for different volumes configuration have not been used in order to extract conductance and transient mass flow rate values when such high initial pressure ratios are imposed (section 3.2.4).

Another possible reason of the small difference between experiments and numerical results could be due to the non-negligible effects of the gas/surface interactions at low rarefaction levels. A non complete accommodation at the wall could play a significant role in the variation of pressure with time, too. Even if it has been found that for this tube the tangential momentum accommo-

dation for nitrogen in the case of metallic surfaces can be slightly less than unity [Silva et al, 2016], the experimental results were compared to BGK results obtained for a tangential accommodation coefficient  $\alpha = 1$ , that is for a complete diffuse gas accommodation at the surface.

## 5.2 Stationary mass flow rate

From the non stationary results obtained it is also possible to extract stationary mass flow rate results by means of the conductance results obtained in Section 4.2. Therefore, we here show results of stationary mass flow rates obtained by using the dynamic constant volume technique and we compare them to results obtained numerically from the BGK model kinetic equation (Graur and Sharipov [2008]).

Let us remember that the conductance, for a fixed tube geometry, varies only as a function of the mean rarefaction (or mean pressure) and of the gas used. This means that the conductance does not depend on the initial pressure difference imposed.

Therefore, in order to extract a stationary mass flow rate, once the conductance has been measured for a

Nitrogen			
$\delta_m$	$C [m^3/s] \times 10^7$	$\delta_m$	$C [m^3/s] \times 10^7$
338.3	32.04	11.06	1.855
276.7	26.35	8.691	1.639
229.4	21.96	7.238	1.517
185.0	17.88	5.968	1.397
153.6	15.04	5.037	1.317
123.2	12.36	4.109	1.237
100.1	10.16	3.746	1.211
83.78	8.650	2.956	1.150
67.36	7.088	2.461	1.127
55.34	5.954	2.031	1.095
45.10	4.994	1.849	1.046
35.87	4.141	1.476	1.036
36.23	4.179	1.155	1.039
29.52	3.552	0.985	1.015
24.20	3.056	0.750	1.033
19.54	2.625	0.632	0.986
16.29	2.332	0.506	0.993
13.73	2.097		

**Table 3** Values of Conductance  $C$  as a function of the mean rarefaction parameter  $\delta_m$  for nitrogen.

given rarefaction condition, one can reduce eq. (22) in the limit of  $t \rightarrow 0$  to

$$\dot{M} = \frac{C}{RT} \Delta p_0, \quad C = f(\delta_m, gas). \quad (24)$$

If one knows the conductance for one precise rarefaction condition, one can obtain the mass flow rate along the tube for an arbitrary difference of pressure imposed. For example, for an experiment performed with nitrogen at an initial pressure difference of  $\Delta p_0 = 133.5 Pa$  and mean rarefaction  $\delta_m = 4.1$ , the conductance obtained was  $C = 12.37 \times 10^{-8} m^3 s^{-1}$  (see Table 3). This conductance value was obtained from one single experiment, nevertheless, with this value it is not only possible to extract the mass flow rate that corresponds to the initial pressure difference of the experiment, but also the mass flow rates for lower or higher pressure differences, as shown in Figure 10.

This property which is characteristic of the conductance parameter is very useful, since normally mass flow rates engendered by very low pressure differences are extremely difficult to measure. Nevertheless, with this technique one could apparently measure mass flow rates at arbitrary pressure differences imposed. The here presented mass flow rate measurements have been calculated for  $\Delta p = 100 Pa$ ,  $\Delta p = 10 Pa$  and  $\Delta p = 1 Pa$ , but other pressure differences could have been used. Moreover, the methodology suffers of no apparent accuracy limitations in within the three order of magnitudes of pressure differences tested. It is possible to observe that

we obtained very stable results that match with great accuracy the numerical results obtained by means of BGK. The uncertainties are the same as the ones declared in Section 4.2 for the conductance measurements.

## 6 Conclusions

This work is a first effort to experimentally analyze transient rarefied gas flows through long tubes. This study is aimed to add knowledge on time-dependent micro gas flows which is at the present moment lacking in the literature. Specific applications of transient micro flows could be applied to gas separators, micro chromatography, oscillating micro actuators and others. Of novelty and particular importance is the new methodology proposed in order to extract from a theoretically derived exponential expression characteristic times of single experiments which can characterize the relaxation phenomenon of pressure variation with time as a function of gas molecular weight and gas rarefaction. **The new methodology differs from the classic constant volume technique since it does not suffer of limitations in respect to the time scale needed in order to perform the measurement: in the classic technique a stationary assumption and a proper time interval were necessary in order to perform stationary mass flow rate measurements. The dynamic methodology can easily perform transient mass flow rate measurements through a micro-device in a stable and repeatable manner. Fur-**



thermore, the technique offers the possibility to associate the characteristic time of the experiment to the conductance of the tube for a given gas. This new methodology could be used as an efficient and real-time micro gas mass flow meter as it allows to measure at any instant transient gas flows that are far lower in dimensions in respect to the measurements performed by mass flow meters that are currently commercially available.

The here proposed study has been conducted for fixed parameters such as the diameter and length of the tube. It was observed that the pressure relaxation phenomenon depends greatly on gas rarefaction and its speed can vary as much as 10 folds from transition to hydrodynamic regime. If different gases are compared at same rarefaction conditions, the lighter gas is always faster to relax to equilibrium in respect to a heavier gas. The mass flow rate variation with time behavior as a function of the gas rarefaction and molecular weight was analyzed, too.

Moreover, the dynamic constant volume technique offers the possibility to extract stationary values of mass flow rate by means of the conductance  $C$ , which was obtained from the time-dependent experiments. It was possible to obtain a large spectrum of results from a reduced number of experiments performed. This final result of the paper represents a significant accomplishment.

Finally, the pressure variation with time experimental results were compared to results obtained from the BGK kinetic model equations and the agreement is excellent for flows in slip and transitional regime while the comparison is good for flow tending towards free molecular regime. To conclude, the stationary experimental results of mass flow rate give an excellent agreement in respect to the BGK kinetic model.

**Acknowledgements** This work has been partially (authors M.-T. Ho and I. Graur) carried out in the framework of the Labex MEC (ANR-10-LABX-0092) and of the A\*MIDEX project (ANR-11-IDEX-0001-02), funded by the "Investissements d'Avenir" French Government program managed by the French National Research Agency (ANR). Additionally, the authors E. Silva and C. J. Deschamps thank the support of EMBRACO, CNPq and EMBRAP II Unit Polo/UFSC.

## References

- Arkilic E, Schmidt M, Breuer K (1997) Gaseous slip flow in long microchannels. *Microelectromechanical Systems, Journal of* 6(2):167–178
- Arkilic EB, Breuer KS, Schmidt MA (2001) Mass flow and tangential momentum accommodation in silicon micromachined channels. *Journal of fluid mechanics* 437:29–43
- Colin S (2005) Rarefaction and compressibility effects on steady and transient gas flows in microchannels. *Microfluidics and Nanofluidics* 1(3):268–279
- Ewart T, Perrier P, Graur I, Gilbert Méolans J (2006) Mass flow rate measurements in gas micro flows. *Experiments in fluids* 41(3):487–498
- Ewart T, Perrier P, Graur I, Méolans J (2007) Tangential momentum accommodation in microtube. *Microfluidics and Nanofluidics* 3(6):689–695
- Graur I, Sharipov F (2008) Gas flow through an elliptical tube over the whole range of the gas rarefaction. *European Journal of Mechanics-B/Fluids* 27(3):335–345
- Harley JC, Huang Y, Bau HH, Zemel JN (1995) Gas flow in micro-channels. *Journal of Fluid Mechanics* 284:257–274
- Jousten K (ed) (2008) *Handbook of Vacuum Technology*. WILEY-VCH Verlag GmBH & Co. KGaA. Weinheim
- Lilnaropoulos J, Valougeorgis D (2011) Unsteady vacuum gas flow in cylindrical tubes. *Fusion Engineering and Design* 86(9):2139–2142
- Perrier P, Graur I, Ewart T, Méolans J (2011) Mass flow rate measurements in microtubes: From hydrodynamic to near free molecular regime. *Physics of Fluids* 23:042,004
- Pitakarnnop J, Varoutis S, Valougeorgis D, Geoffroy S, Baldas L, Colin S (2010) A novel experimental setup for gas microflows. *Microfluidics and Nanofluidics* 8(1):57–72
- Porodnov B, Suetin P, Borisov S, Akinshin V (1974) Experimental investigation of rarefied gas flow in different channels. *Journal of fluid mechanics* 64(3):417–437
- Rojas-Cardenas M, Graur I, Perrier P, Meolans JG (2011) Thermal transpiration flow: a circular cross-section microtube submitted to a temperature gradient. *Physics of Fluids* 23:031,702
- Sharipov F (1997) Rarefied gas flow through a long tube at arbitrary pressure and temperature drop. *J Vac Sci Technol A* 15(4):2434–2436
- Sharipov F (2011) Data on the velocity slip and temperature jump on a gas-solid interface. *Journal of Physical and Chemical Reference Data* 40(2):023,101
- Sharipov F (2012a) Benchmark problems in rarefied gas dynamics. *Vacuum* 86(11):1697–1700
- Sharipov F (2012b) Transient flow of rarefied gas through an orifice. *Journal of Vacuum Science & Technology A* 30(2):021,602
- Sharipov F (2013) Transient flow of rarefied gas through a short tube. *Vacuum* 90:25–30
- Sharipov F, Graur I (2014) General approach to transient flows of rarefied gases through long capillaries.

1 Vacuum 100:22–25

2 Sharipov F, Graur I, Day C (2010) Leak rate of water  
3 into vacuum through microtubes. *Journal of Vac Sci*  
4 *Technol A* 28(3):443–448

5  
6 Silva E, Rojas-Cardenas M, Deschamps C (2016) Ex-  
7 perimental analysis of velocity slip at the wall for gas  
8 flows of nitrogen, r134a, and r600a through a metal-  
9 lic microtube. *International Journal of Refrigeration*  
10 Accepted

11 Vargas M, Naris S, Valougeorgis D, Pantazis S, Jousten  
12 K (2014a) Hybrid modeling of time-dependent rar-  
13 eified gas expansion. *Journal of Vacuum Science &*  
14 *Technology A* 32(2):021,602

15 Vargas M, Naris S, Valougeorgis D, Pantazis S, Jousten  
16 K (2014b) Time-dependent rarefied gas flow of single  
17 gases and binary gas mixtures into vacuum. *Vacuum*  
18 109:385–396

19 Yamaguchi H, Hanawa T, Yamamoto O, Matsuda Y,  
20 Egami Y, Niimi T (2011) Experimental measurement  
21 on tangential momentum accommodation coefficient  
22 in a single microtube. *Microfluidics and nanofluidics*  
23 11(1):57–64  
24  
25  
26  
27  
28  
29  
30  
31  
32  
33  
34  
35  
36  
37  
38  
39  
40  
41  
42  
43  
44  
45  
46  
47  
48  
49  
50  
51  
52  
53  
54  
55  
56  
57  
58  
59  
60  
61  
62  
63  
64  
65